IOP Publishing Physica Scripta
Phys. Scr. 95 (2020) 025206 (7pp) https://doi.org/10.1088/1402-4896/ab43ff

Mathematical model for blood flow through the stenosed channel

Azad Hussain[1,3], Lubna Sarwar[1], Sobia Akbar[1] and Sohail Nadeem[2]

[1] Department of Mathematics, University of Gujrat, Gujrat 50700, Pakistan
[2] Department of Mathematics, Quaid-I-Azam University, Islamabad 44000, Pakistan

E-mail: azad.hussain@uog.edu.pk

Received 27 May 2019, revised 29 August 2019
Accepted for publication 12 September 2019
Published 31 December 2019

Abstract

In this paper, we investigate the blood flow through a stenoised channel. In current study Cartesian coordinates are contemplated for flow in the channel and in an axisymmetric tube with transfer of heat having cosine shape stenosis. Blood is supposed as Eyring–Powell fluid which is independent of time. Thermal conductivity is determined by temperature. After assimilating these deliberations, dimensional equations are transformed into non-dimensional system of differential equations with the use of similarity transformations and are then solved numerically. A parametric study is executed to depict the impact of various parameters on the velocity and temperature fields of fluid. Heat transfer coefficient and skin friction are also explained through graphs and discussed in tabular form for distinct values of dimensionless parameters. The current investigation tells that velocity field significantly increases by rising the value of M and δ. Temperature field $\theta(\eta)$ increases for extended value of δ, M, K, B, A and Pr. Nusselt number curve increases due to increase in Pr.

Keywords: Eyring–Powell fluid model, blood flow, heat transfer, numerical solution, stenosed channel

(Some figures may appear in colour only in the online journal)

1. Introduction

Blood is an important fluid of our body, like other bio-fluids. The study of blood flow in blood vessels such as arteries and veins under the effect of stenosis has been a topic of long-standing interest for researchers [1–5]. Today, we can see that arteries are choked because of modern lifestyles, high blood cholesterol, smoking and possibly a genetic problem. Blood circulation executes different function types in a human body such as oxygen transportation, transport of nutrients, ejection of carbon dioxide and deportation of metabolic products. There are three types of blood circulation namely micro-circulation, systemic circulation and capillary circulation. Experientially, it has been proven that blood is the suspension of red blood cells, white blood cells, and platelets. Newtonian behavior of blood is acceptable for high shear rate flow i.e. when blood flow through larger area arteries and is non-Newtonian when the shear rate is below i.e. flowing through smaller area arteries, veins and in the downstream of the stenosis. It has been observed that blood shows momentous non-Newtonian properties in some diseased conditions since it is observed through experiments that most of the biological fluids express rheology of non-Newtonian aspects. The most prestigious equations known as Navier–Stokes can not explain the attributes of non-Newtonian fluid models. Therefore, several intrinsic equations for non-Newtonian fluid models have been carried out with the character of the density of the fluid. Non-Newtonian fluids have a lot of applications in industry, medical field and engineering sciences. In modeling of steel substances, petroleum drilling, expulsion of polymers, and demolishing of glasses, non-Newtonian fluids have emerging applications. Some polymers are utilized in communication, agriculture, medical appliances. Due to lot of applications in industry and medicine, the investigation of non-Newtonian fluids is a topic of great interest to modern researchers [6–14]. Erying and Powell [15] developed a fluid model having nature of non-Newtonian fluid models. The Eyring–Powell fluid is very complicated mathematical model but it fascinates the researchers attention due to the its advantages over the power law model. This fluid model contains many beneficial approaches in the field of fluids. First of all it is originated from kinetic theory of

[3] Author to whom any correspondence should be addressed.

liquids and having no connection with empirical relation. Secondly it can be used for Newtonian behavior at low and high values of shear rates [16]. By literature review [17–19] many mathematicians paid attention towards the study of Eyring–Powell fluid.

In current analysis, the blood is considered to be Eyring–Powell fluid in the stenosis and the attained governing equations are presented in the form of stream function as a compatibility equation. The analysis of the existing literature suggests that to the best of the author's knowledge, no studies have been reported regarding the Eyring–Powell model fluid through stenoised artery.

2. Mathematical equations

The Eyring–Powell model fluid stress tensor which is

$$\tau = \mu\nabla v + \frac{1}{\beta}\sinh^{-1}\left(\frac{1}{D}\nabla v\right), \tag{1}$$

where τ indicates the cauchy stress tensor, v illustrates the velocity, μ indicates viscosity, and D shows the material constant,

$$\sinh^{-1}\left(\frac{1}{D}\nabla v\right) \approx \frac{1}{D}\nabla v - \frac{1}{6}\left(\frac{1}{D}\nabla v\right)^3, \quad \left|\frac{1}{D}\nabla v\right| \ll 1. \tag{2}$$

3. Mathematical formulation

Assuming the flow of steady, homogenous and incompressible Eyring–Powell fluid (assumed as blood) via two dimensional stenoised channel of length $\frac{l_0}{2}$. The coordinates are considered in such a manner that the arterial system lies in the *xy-plane* such that *x-axis* concurs with the axis in the direction of the flow and *y-axis* is taken normal to *x-axis*.

In schematic diagram of the problem, $\boldsymbol{\lambda}$ is the maximum height of the stenosis, $h(x)$ is the space in the stenosed area and $2h_0$ is the breadth of the unimpeded channel.

Boundary of stenosed region is chosen as

$$\begin{aligned} h(x) &= h_0 - \frac{\lambda}{2}\left(1 + \mathrm{Cos}\left(\frac{4\pi x}{l_0}\right)\right), \quad -\frac{l_0}{4} < x < \frac{l_0}{4} \\ &= h_0 \qquad\qquad\qquad\qquad \text{Otherwise.} \end{aligned} \tag{3}$$

3.1. Governing equations

The governing equations are [20]

$$\vec{\nabla}\vec{V} = 0, \tag{4}$$

$$\rho\frac{\mathrm{d}\vec{V}}{\mathrm{d}t} = \vec{\nabla}\vec{\tau} + \rho b, \tag{5}$$

$$\rho C_p\frac{\mathrm{d}T}{\mathrm{d}t} = \mathrm{k}\nabla^2\mathrm{T} + \varphi, \tag{6}$$

$$\varphi = \tau\nabla V, \tag{7}$$

where ρ shows density of fluid, C_p specific heat, k thermal conductivity, b body force, ∇ is the Laplacian and φ is the dissipation function. For incompressible Eyring–Powell model fluid the continuity equation becomes

$$\frac{\partial u}{\partial x} + \frac{\partial v}{\partial y} = 0. \tag{8}$$

The momentum equation becomes

$$\begin{aligned} \left(u\frac{\partial u}{\partial x} + v\frac{\partial u}{\partial y}\right) &= -\frac{1}{\rho}\frac{\partial p}{\partial x} + 2\nu\frac{\partial^2 u}{\partial x^2} + \frac{2}{\rho\beta C}\frac{\partial^2 u}{\partial x^2} \\ &- \frac{4}{3\rho\beta C^3}\frac{\partial}{\partial x}\left(\frac{\partial u}{\partial x}\right)^3 - \frac{2}{3\rho\beta C^3}\frac{\partial}{\partial x}\left(\frac{\partial u}{\partial x}\right)\left(\frac{\partial u}{\partial y} + \frac{\partial v}{\partial x}\right)^2 \\ &+ \left(\nu + \frac{1}{\rho\beta C}\right)\frac{\partial^2 u}{\partial y^2} - \frac{2}{3\rho\beta C^3}\frac{\partial}{\partial y}\left(\frac{\partial u}{\partial x}\right)^2\left(\frac{\partial u}{\partial y} + \frac{\partial v}{\partial x}\right) \\ &- \frac{1}{6\rho\beta C^3}\frac{\partial}{\partial y}\left(\frac{\partial u}{\partial y} + \frac{\partial v}{\partial x}\right)^3, \end{aligned} \tag{9}$$

$$\begin{aligned} \left(u\frac{\partial v}{\partial x} + v\frac{\partial v}{\partial y}\right) &= -\frac{1}{\rho}\frac{\partial p}{\partial y} - \frac{1}{3\rho\beta C^3}\frac{\partial}{\partial y}\left(\frac{\partial u}{\partial x}\left(\frac{\partial u}{\partial y} + \frac{\partial v}{\partial x}\right)^2\right) \\ &+ \left(\nu + \frac{1}{\rho\beta C}\right)\frac{\partial}{\partial x}\left(\frac{\partial u}{\partial y} + \frac{\partial v}{\partial x}\right) \\ &- \frac{2}{3\rho\beta C^3}\frac{\partial}{\partial x} \times \left(\frac{\partial u}{\partial x}\right)^2\left(\frac{\partial u}{\partial y} + \frac{\partial v}{\partial x}\right) - \frac{1}{6\rho\beta C^3} \\ &\times \frac{\partial}{\partial x}\left(\frac{\partial u}{\partial y} + \frac{\partial v}{\partial x}\right)^3. \end{aligned} \tag{10}$$

The obtained energy equation is

$$\begin{aligned} \rho C_p\left(u\frac{\partial}{\partial x} + v\frac{\partial}{\partial y}\right)T &= k\left(\frac{\partial^2}{\partial x^2} + \frac{\partial^2}{\partial y^2}\right)T - p\frac{\partial u}{\partial x} \\ &+ 2\left(\mu + \frac{1}{\beta C}\right)\left(\frac{\partial u}{\partial x}\right)^2 - \frac{4}{3\beta C^3}\left(\frac{\partial u}{\partial x}\right)^4 - \frac{4}{3\beta C^3} \\ &\times \left(\frac{\partial u}{\partial x}\right)^2\left(\frac{\partial u}{\partial y} + \frac{\partial v}{\partial x}\right)^2 + \left(\mu + \frac{1}{\beta C}\right)\left(\frac{\partial u}{\partial y} + \frac{\partial v}{\partial x}\right)^2 \\ &- \frac{1}{6\rho\beta C^3}\left(\frac{\partial u}{\partial y} + \frac{\partial v}{\partial x}\right)^4, \end{aligned} \tag{11}$$

where C_p represents the specific heat of fluid.

Under above conditions the boundary layer equations for steady incompressible flow towards a stenoised region become:

$$\begin{aligned} \left(u\frac{\partial u}{\partial x} + v\frac{\partial u}{\partial y}\right) &= -\frac{1}{\rho}\frac{\partial p}{\partial x} - \frac{8}{3\rho\beta C^3}\left(\frac{\partial u}{\partial x}\right)\left(\frac{\partial u}{\partial y}\right)\left(\frac{\partial^2 u}{\partial x\partial y}\right) \\ &+ \left(\nu + \frac{1}{\rho\beta C}\right)\frac{\partial^2 u}{\partial y^2} - \frac{2}{3\rho\beta C^3}\left[\left(\frac{\partial u}{\partial x}\right)^2\frac{\partial^2 u}{\partial y^2}\right. \\ &\left. + \left(\frac{\partial u}{\partial y}\right)^2\left(\frac{\partial^2 u}{\partial x^2}\right)\right], \end{aligned} \tag{12}$$

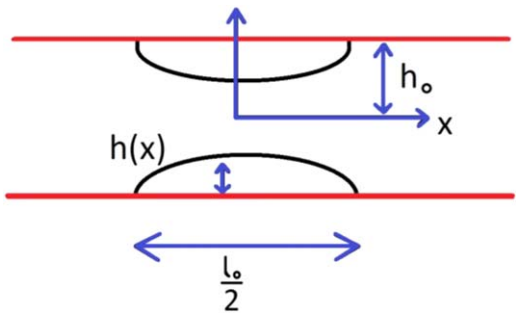

Figure 1. Schematic diagram of the problem.

$$-\frac{1}{\rho}\frac{\partial p}{\partial y} = 0, \tag{13}$$

$$\nu\frac{\partial T}{\partial y} = \frac{k}{\rho C_p}\frac{\partial^2 T}{\partial y^2} - \frac{4}{3\rho C_p \beta C^3}\left(\frac{\partial u}{\partial x}\right)^2\left(\frac{\partial u}{\partial y}\right)^2 + \left(\frac{\nu}{C_p} + \frac{1}{\rho C_p \beta C}\right)\left(\frac{\partial u}{\partial y}\right)^2. \tag{14}$$

According to the configuration of the problem in figure 1 the suitable boundary conditions are,

$$u = v = 0,\ \frac{\partial u}{\partial y} = 0\ at\ y = h(x),$$
$$T = T_1,\quad \frac{\partial T}{\partial y} = 0\ at\ y = 0. \tag{15}$$

3.2. Solution of the problem

The continuity equation is automatically satisfied by introducing the relation for u and v in the form of stream function as:

$$u = \frac{\partial \psi}{\partial y},\ v = -\delta\frac{\partial \psi}{\partial x}, \tag{16}$$

For relations (16), equation (2) is satisfied automatically and the equations (12) and (14) take the following form:

$$\frac{\partial \psi}{\partial y}\frac{\partial^2 \psi}{\partial x \partial y} - \delta\frac{\partial \psi}{\partial x}\frac{\partial^2 \psi}{\partial y^2} = -\frac{8}{3\rho\beta C^3}\frac{\partial^2 \psi}{\partial y^2}\frac{\partial^2 \psi}{\partial x \partial y}\frac{\partial^3 \psi}{\partial x \partial y^2} + \left(\nu + \frac{1}{\rho\beta C}\right)\frac{\partial^3 \psi}{\partial y^3} - \frac{2}{3\rho\beta C^3}\left[\frac{\partial^3 \psi}{\partial y^3}\left(\frac{\partial^2 \psi}{\partial x \partial y}\right)^2 + \left(\frac{\partial^2 \psi}{\partial y^2}\right)^2\frac{\partial^3 \psi}{\partial x^2 \partial y}\right], \tag{17}$$

$$-\delta\frac{\partial \psi}{\partial x}\frac{\partial T}{\partial y} = \frac{k}{\rho C_p}\frac{\partial^2 T}{\partial y^2} - \frac{4}{3\rho C_p \beta C^3}\left(\frac{\partial^2 \psi}{\partial x \partial y}\right)^2\left(\frac{\partial^2 \psi}{\partial y^2}\right)^2 + \left(\frac{\nu}{C_p} + \frac{1}{\rho C_p \beta C}\right)\left(\frac{\partial^2 \psi}{\partial y^2}\right)^2. \tag{18}$$

The boundary conditions are reduced to:

$$\psi = \frac{1}{2},\ T = T_1 \text{ at } y = f,$$
$$\frac{\partial \psi}{\partial x} = 0,\ \psi = 0,\ T = T_1 \text{ at } y = 0. \tag{19}$$

Now to convert these equations in single variable, introducing the stream function as follows:

$$\psi = \sqrt{a\nu}\, x f(\eta), \tag{20}$$

where the similarity variable η is given by $\eta = y\sqrt{\frac{a}{\nu}}$.

Using relation (20), equation (17) finally, has the following form:

$$(1 + M)f''' - \frac{2}{3}GMf'(f'f''' + 4f''^2) + \delta f''f - f'^2 = 0. \tag{21}$$

Next, the dimensionless temperature θ is introduced as:

$$\theta(\eta) = \frac{T - T_0}{T_1 - T_0}. \tag{22}$$

By using equation (20) and similarity variable equation (18) reduces to:

$$\theta'' - \frac{8}{3}MKB\theta f'^2 f''^2 + (1 + M)A\theta f''^2 + \delta Pr\theta' f = 0, \tag{23}$$

where

$$Pr = \frac{C_p\mu}{k},\ A = \frac{\mu a^2 x^2}{k},\ M = \frac{1}{\mu\beta C},\ B = \frac{a\mu^2}{k\rho},$$
$$G = \frac{a^3 x^2}{2\nu C^2}. \tag{24}$$

The dimensionless boundary conditions are

$$f(0) = 0,\ f(b) = \frac{1}{2},\ f'(b) = 0\ at\ b = f\sqrt{\frac{a}{\nu}}, \tag{25}$$
$$\theta(b) = 1,\ \theta(0) = 0. \tag{26}$$

The interesting physical objects i.e. Nusselt number and Skin friction of the flow field are also obtained.

4. Graphical results and discussion

Impact of physical parameters on velocity and temperature fields is explained with the assistance of tables and graphs. Figure 1 shows the schematics diagram of the problem. Figure 2 tells the impact of A on temperature field. The relationship between temperature and A is directly proportional. Temperature profile increases for increasing value of A. Figure 3 demonstrates the instance of B on temperature profile. The temperature field shows increasing behavior due to increase in the value of B. Figure 4 explores the behavior of δ on temperature profile. The temperature field increases by raising δ. Figure 5 draws the consequences of k on temperature distribution. Figure 6 illuminates the behavior of M on

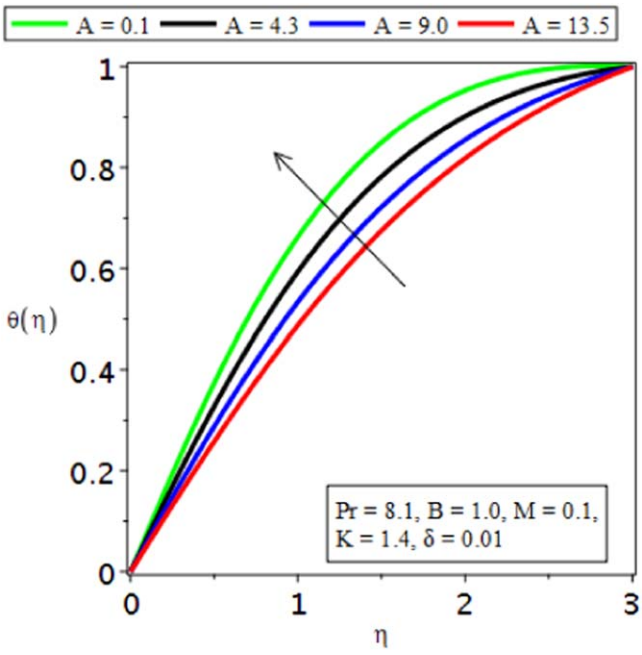

Figure 2. Impact of A on temperature profile.

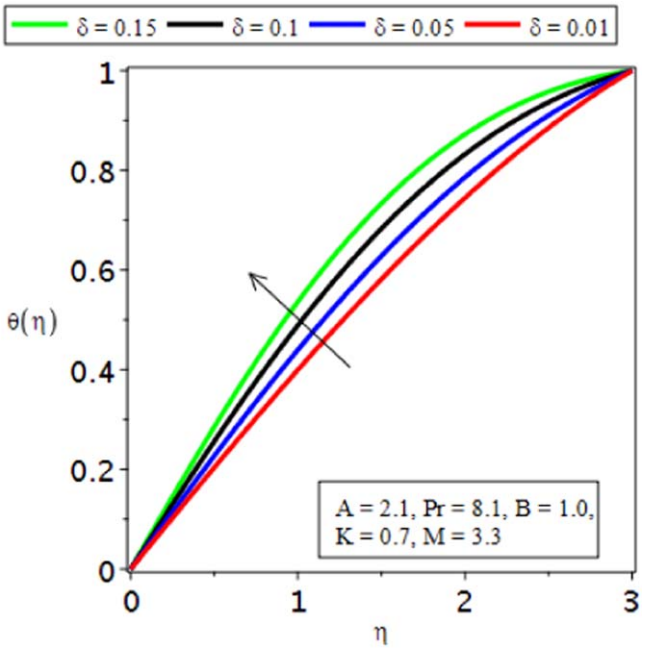

Figure 4. Response of δ on temperature field.

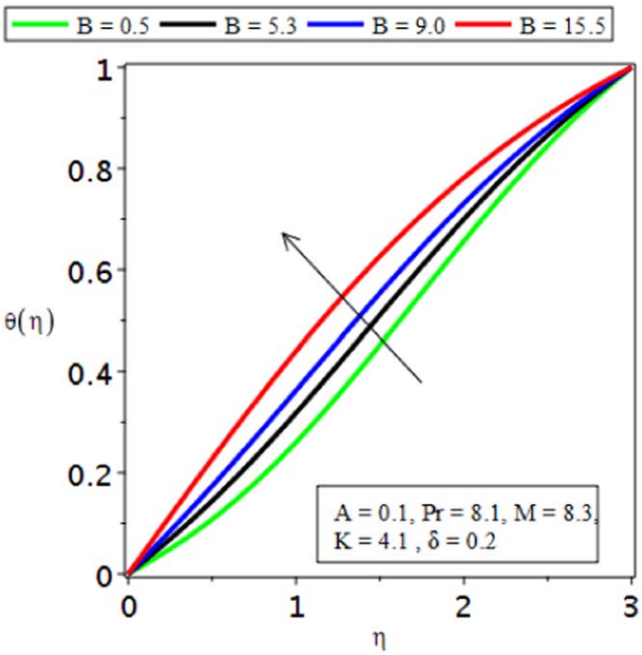

Figure 3. Consequences of B on temperature field.

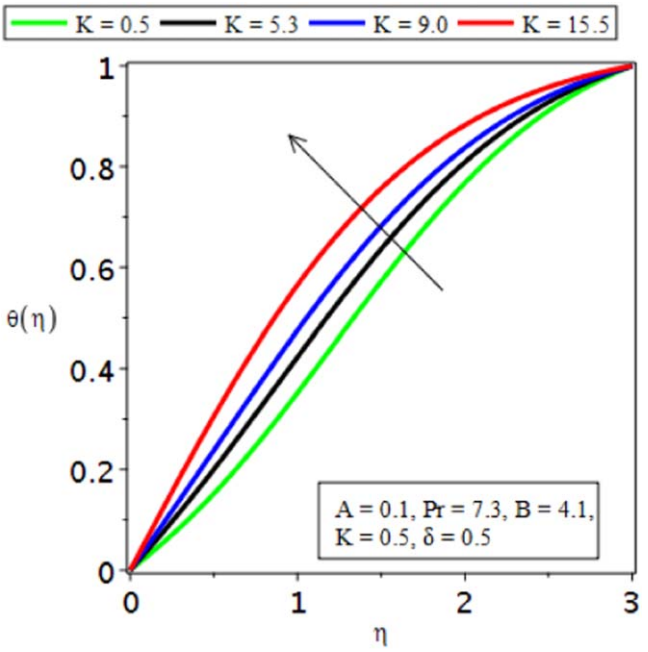

Figure 5. Impact of K on temperature field.

temperature field. The temperature profile rises by changing the values of M. Figure 7 describes the Pr behavior on temperature profile. Temperature curve increases due to increase in Pr. Figures 8–9 shows the impact δ and M on velocity profile, respectively. Velocity curves increases by increasing the values of δ and M. Figure 10 shows the variations in heat transfer coefficient by increasing the Pr. Figure 11 draws the consequences of skin friction. Table 1 describes the performance of different parameters on $\theta'(0)$. Values of $\theta'(0)$ decreases due to enhances the values of Pr and δ. Table 2 investigates the results of Pr and δ on heat transfer coefficient. Values of coefficient shows growing behavior owing to rise in parameter δ and shows negative variation by changing the value of Pr. Table 3 express the behavior of β and δ on skin friction. It exhibits positive response for skin friction coefficient when δ increases while by accelerating the values of β the values of skin friction coefficient manifests reducing reaction.

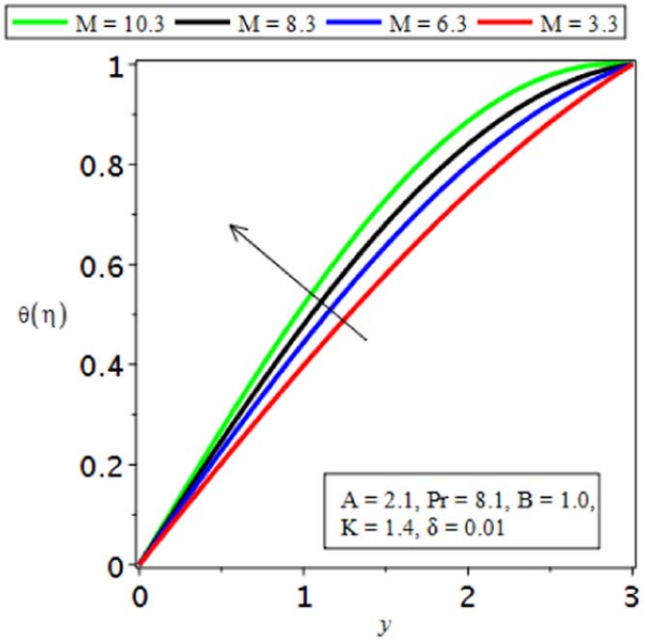

Figure 6. Consequences of M on temperature distribution.

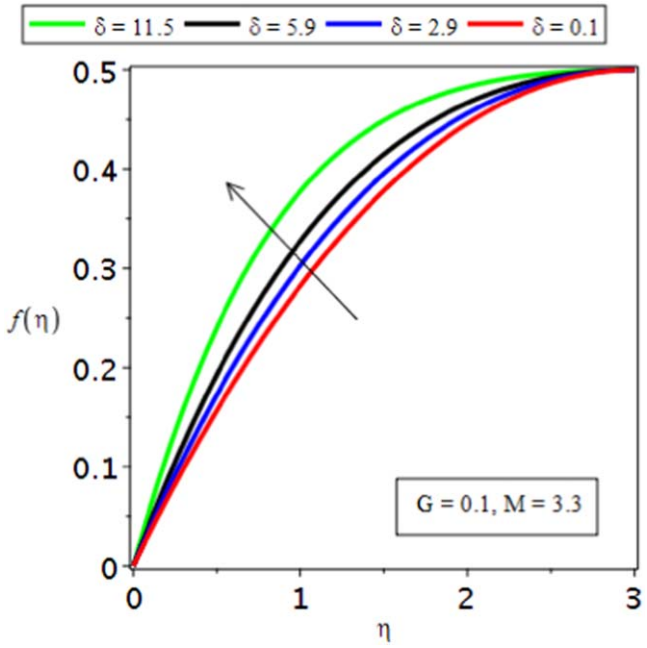

Figure 8. Impact of δ on $f(\eta)$.

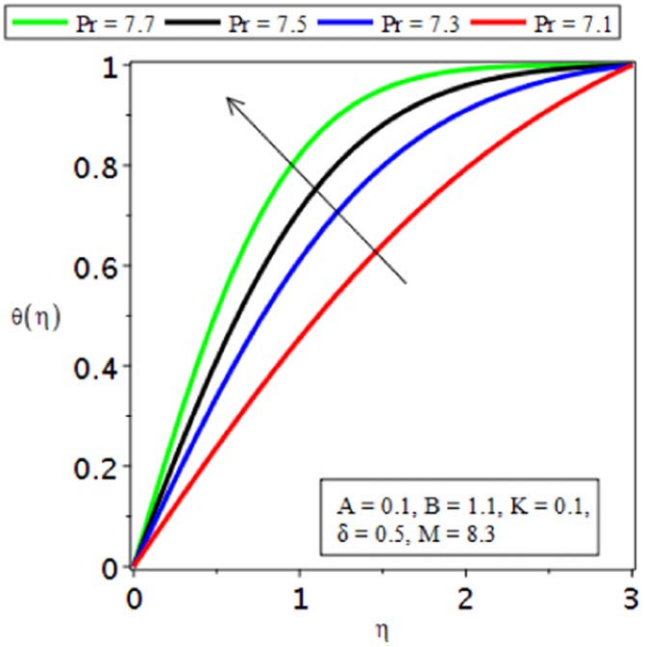

Figure 7. Temperature distribution for values of Pr.

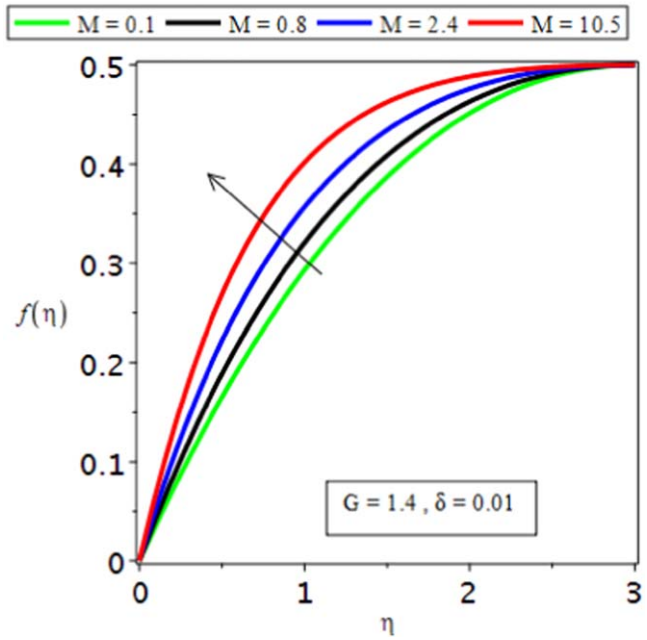

Figure 9. Effects of M on $f(\eta)$.

5. Concluding remarks

A problem of steady state incompressible boundary layer flow of Eyring–Powell fluid in arterial stenosis has been investigated. By using the useful similarity transformations we transformed the PDE into ODE's. Results of distinctive parameters of velocity and temperature fields were obtained about the influence of fluids flow. The desired phenomenon has been explained with the assistance of graphs and tables. The main results are:

(1) Temperature field $\theta(\eta)$ increases for extended value of δ, M, K, B, A and Pr.
(2) Velocity curve $\theta(\eta)$ increases for expanding values of δ and M.
(3) Nusselt number curve Nu profile-rates owing to increment in the value of Pr.
(4) Temperature has been found to decrease due to enlargement in M and δ.

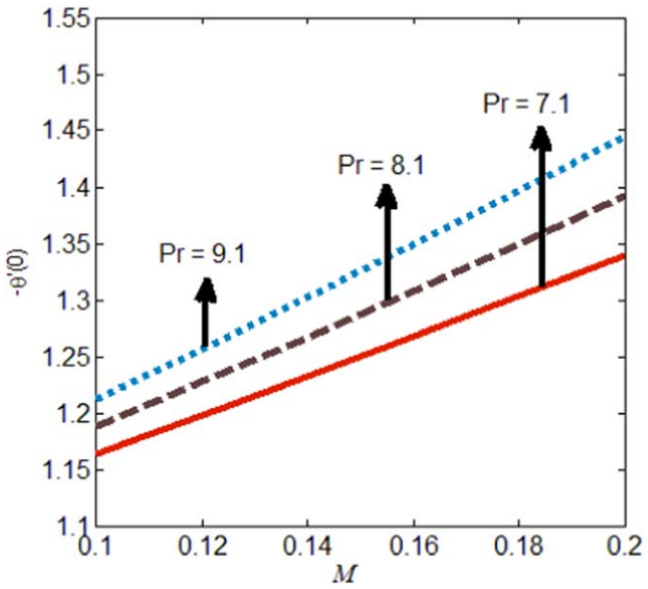

Figure 10. Nusselt number variations $-\theta'(0)$ for distinct values of Pr and M.

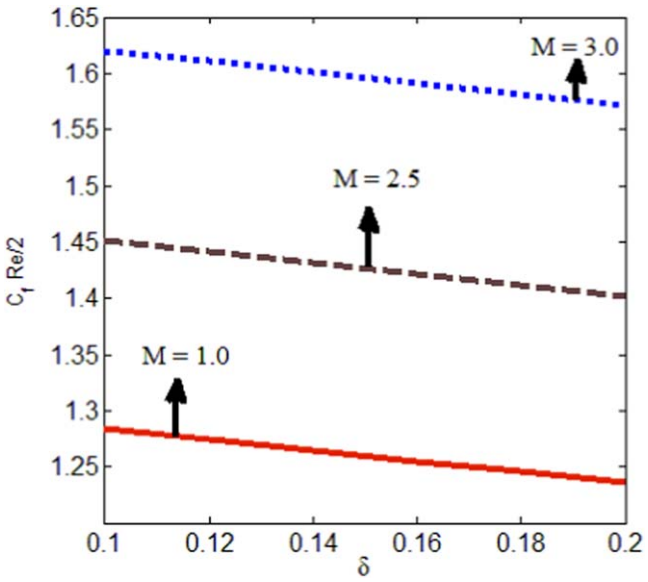

Figure 11. Values of skin friction for M and δ.

Table 1. Values of $\theta'(0)$ at the wall for δ, M, K, B, A and Pr.

δ	0.01	0.05	0.1	0.15
A				
M				
Pr	0.410 23	0.459 13	0.521 30	0.583 61
B				
K				
Pr	7.1	7.3	7.5	7.7
A				
M				
δ	0.482 47	0.701 63	0.839 65	0.851 56
B				
K				
A	0.1	4.3	9.0	13.5
Pr				
M				
δ	0.527 44	0.594 13	0.683 33	0.787 26
B				
K				

Table 2. Values of Nusselt number $-\theta'(0)$ for M and Pr.

M	Pr	$-\theta'(0)$
0.1	7.1	−0.834 98
0.12		−0.834 50
0.14		−0.834 03
0.1		−0.834 98
	7.15	−0.838 20
	7.2	−0.841 42

Table 3. Values of skin friction coefficient for M and Pr.

δ	M	$\frac{1}{2}C_f Re$
0.1	0.3	0.380 29
0.12		0.381 31
0.14		0.382 33
0.1		0.380 29
	0.4	0.378 13
	0.5	0.378 30

ORCID iDs

Azad Hussain https://orcid.org/0000-0002-3100-582X

References

[1] Ellahi R, Zeeshan A, Hussain F and Asadollahi A 2019 Peristaltic blood flow of couple stress fluid suspended with nanoparticles under the influence of chemical reaction and activation energy *Symmetry* **11** 276
[2] Bhatti M M, Zeeshan A and Ellahi R 2016 Endoscope analysis on peristaltic blood flow of Sisko fluid with Titanium magneto-nanoparticles *Comput. Biol. Med.* **78** 29–41
[3] Bhatti M M, Zeeshan A and Ellahi R 2016 Heat transfer analysis on Peristaltically induced motion of particle-fluid suspension with variable viscosity: clot blood model *Comput. Methods Prog. Biomed.* **137** 115–24
[4] Prakash J, Tripathi D, Tiwari A K, Sait S M and Ellahi R 2019 Peristaltic pumping of nanofluids through tapered channel in porous environment: applications in blood flow *Symmetry* **11** 868

[5] Ellahi R, Rahman S U and Nadeem S 2014 Blood flow of Jeffrey fluid in a catherized tapered artery with the suspension of nanoparticles *Phys. Lett.* A **378** 2973–80
[6] Ellahi R, Raza M and Vafai K 2012 Series solutions of non-Newtonian nanofluids with Reynolds' model and Vogel's model by means of the homotopy analysis method *Math. Comput. Modell.* **55** 1876–91
[7] Khan M, Malik M Y, Salahuddin T and Khan I 2016 Heat transfer squeezed flow of Carreau fluid over a sensor surface with variable thermal conductivity, a numerical study *Results Phys.* **6** 940–5
[8] Hussain A, Malik M Y, Salahuddin T, Bilal S and Awais M 2017 Combined effects of viscous dissipation and Joule heating on MHD Sisko nanofluid over a stretching cylinder *J. Mol. Liq.* **231** 341–52
[9] Hussain A, Sarwar L, Nadeem S, Akbar S and Jamal S Inquisition of combined effects of radiation and MHD on elasticoviscous fluid flow past a pervious plate *J. Braz. Soc. Mech. Sci. Eng.* **40** 343
[10] Salahuddin T, Malik M Y, Hussain A, Awais M, Khan I and Khan M 2017 Analysis of tangent hyperbolic nanofluid impinging on a stretching cylinder near the stagnation point *Results Phys.* **7** 426–34
[11] Hussain A, Malik M Y, Bilal S, Awais M and Salahuddin T 2017 Computational analysis of magnetohydrodynamic Sisko fluid flow over a stretching cylinder in the presence of viscous dissipation and temperature dependent thermal conductivity *Results Phys.* **7** 139–46
[12] Hussain A, Ghafoor S, Malik M Y and Jamal S 2017 An exploration of viscosity models in the realm of kinetic theory of liquids originated fluids *Results Phys.* **7** 2352–60
[13] Hussain A, Sarwar L, Akbar S, Malik M Y and Ghafoor S 2018 Model for MHD viscoelastic nanofluid flow with prominence effects of radiation *Heat Transfer-Asian Res.* **12** 463–82
[14] Abdullah B, Alzahrani K and Alshomrani A S 2019 Numerical analysis in mathematical modelling for mixed convection flow with radiative heat transfer *Phys. Scr.* **94** 11
[15] Powell R E and Eyring H 1944 Mechanism for relaxation theory of viscosity *Nature* **7** 427–8
[16] Nadeem S and Saleem S 2014 Mixed convection flow of Eyring–Powell fluid along a rotating cone *Results Phys.* **4** 54–62
[17] Akbar N S and Nadeem S 2012 Characteristics of heating scheme and mass transfer on the peristaltic flow for an Eyring–Powell fluid in an endoscope *Int. J. Heat Mass Transf.* **55** 375–83
[18] Rehman A, Achakzi S, Nadeem S and Iqbal S 2016 Stagnation point flow of Eyring Powell fluid in a vertical cylinder with heat transfer *J. Power Technol.* **96** 57–62
[19] Khan I, Malik M Y, Salahuddin T, Khan M and Rehman K 2017 Homogenous–heterogeneous reactions in MHD flow of Powell—Eyring fluid over a stretching sheet with Newtonian heating *Neural Comput. Appl.* **30** 3581–8
[20] Siddiqui A M, Haroon T, Mirza A A and Ansari A R 2013 Steady non isothermal two-dimensional flow of newtonian fluid in a stenosed channel *Theory Appl.Math. Comput. Sci.* **3** 75–92